Article

Synthesis and Characterization of Thermoreversible Biopolymer Microgels Based on Hydrogen Bonded Nucleobase Pairing

Rong Cao, Zhenyu Gu, Lorraine Hsu, Gary D. Patterson, and Bruce A. Armitage

J. Am. Chem. Soc., **2003**, 125 (34), 10250-10256• DOI: 10.1021/ja035211t • Publication Date (Web): 31 July 2003

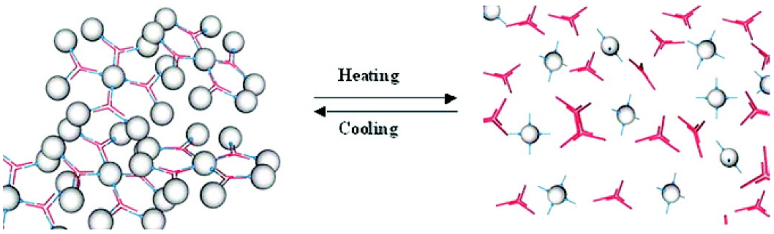

More About This Article

Additional resources and features associated with this article are available within the HTML version:

- Supporting Information
- Links to the 2 articles that cite this article, as of the time of this article download
- Access to high resolution figures
- Links to articles and content related to this article
- Copyright permission to reproduce figures and/or text from this article

View the Full Text HTML

J|A|C|S
ARTICLES
Published on Web 07/31/2003

Synthesis and Characterization of Thermoreversible Biopolymer Microgels Based on Hydrogen Bonded Nucleobase Pairing

Rong Cao, Zhenyu Gu, Lorraine Hsu, Gary D. Patterson, and Bruce A. Armitage*

Contribution from the Department of Chemistry, Carnegie Mellon University, 4400 Fifth Avenue, Pittsburgh, Pennsylvania 15213-3890

Received March 18, 2003; E-mail: army@cyrus.andrew.cmu.edu

Abstract: We describe the synthesis and characterization of a thermoreversibly cross-linked biopolymer microgel based on protein, DNA, and peptide nucleic acid (PNA) components. The DNA assembles into a trifunctional three-way junction (TWJ) with single-stranded overhangs. PNA oligomers complementary to these overhangs and bearing terminal biotin groups hybridize to the DNA TWJ and simultaneously bind to the tetrafunctional protein avidin, leading to a cross-linked system. Dynamic light scattering experiments reveal that micron-sized particles are formed. Static light scattering was used to characterize the internal structure of these microgels, which were found to have a fractal dimension of 1.85, indicative of a loose network structure. Heating disrupts the weakest component in the system, namely the PNA−DNA hybrid, resulting in dissolution of the microgel, while cooling restores the hydrogen bonding leading to reassembly of the microgel. Variation of the nucleotide sequence permits tuning of the gelation temperature with fine control.

Introduction

Polymer gels have been intensively studied due to their intermediate properties between those of the liquid and solid states.[1−3] A gel typically forms when molecular or macromolecular species in solution become cross-linked into network structures. Gels are unique in that they do not flow under the force of gravity, even though solvent is the major component of the material. Of particular interest are gels that respond to changes in the environment, such as temperature or pH.[4−6] These "smart materials" have great potential for a wide variety of applications including cell- and tissue-selective drug delivery and sensing devices.

Gels can be classified as chemical or physical, depending on whether the linkages stabilizing the gel are covalent or noncovalent, respectively. Physical gels hold considerable appeal due to the fact that noncovalent forces are relatively weak, allowing the cross-links to form in reversible fashion.[7,8] This feature is often noted in designs of supramolecular assemblies, where the reversibility of the bonding permits annealing of defects during the formation process.[9,10] Since physical gelation is a supramolecular assembly process, it should be possible to form cross-linked networks having relatively few defects.[11,12]

This report describes the synthesis and characterization of a novel physical gel in which the cross-links stabilizing the supramolecular structure are based on Watson−Crick hydrogen bonded base pairing. Specifically, DNA and a synthetic analogue known as PNA (for peptide nucleic acid) are used to assemble physical gels from the protein avidin. Our goals were to (*i*) assemble these structures in a controlled, thermoreversible fashion, (*ii*) demonstrate fine control over the gelation temperature, and (*iii*) characterize the internal structure of the resulting gels. Biomolecular recognition schemes such as this have been used to assemble network structures previously.[13−20] In one example, Mirkin, Letsinger, and co-workers have developed strategies for functionalizing gold or semiconductor nanoparticles with DNA oligonucleotides.[13,15] Each nanoparticle bears several copies of the DNA strand. In a typical experiment, two

(1) Narita, T.; Knaebel, A.; Munch, J. P.; Candau, S. J. *Macromolecules* **2001**, *34*, 8224−8231.
(2) Semenov, A. N.; Rubinstein, M. *Macromolecules* **2002**, *35*, 4821−4837.
(3) Tsujimoto, M.; Shibayama, M. *Macromolecules* **2002**, *35*, 1342−1347.
(4) Sato, Y.; Hashidzume, A.; Morishima, Y. *Macromolecules* **2001**, *34*, 6121−6130.
(5) Chen, S. J.; Berry, G. C.; Plazek, D. J. *Macromolecules* **1995**, *28*, 6539−6550.
(6) Neumann, B. *J. Phys. Chem. B* **2001**, *105*, 8268−8274.
(7) Shay, J. S.; Raghavan, S. R.; Khan, S. A. *J. Rheol.* **2001**, *45*, 913−927.
(8) Takeshita, H.; Kanaya, T.; Nishida, K.; Kaji, K. *Macromolecules* **2001**, *34*, 7894−7898.
(9) Lehn, J.-M. *Supramolecular Chemistry: Concepts and Perspectives*; VCH: Weinheim, 1995.
(10) Whitesides, G. M.; Simanek, E. E.; Mathias, J. P.; Seto, C. T.; Chin, D. N.; Mammen, M.; Gordon, D. M. *Acc. Chem. Res.* **1995**, *28*, 37−44.
(11) Jeong, B.; Bae, Y. H.; Kim, S. W. *Macromolecules* **1999**, *32*, 7064−7069.
(12) Yamauchi, K.; Lizotte, J. R.; Hercules, D. M.; Vergne, M. J.; Long, T. E. *J. Am. Chem. Soc.* **2002**, *124*, 8599−8604.
(13) Mirkin, C. A.; Letsinger, R. L.; Mucic, R. C.; Storhoff, J. J. *Nature* **1996**, *382*, 607−609.
(14) Petka, W. A.; Harden, J. L.; McGrath, K. P.; Wirtz, D.; Tirrell, D. A. *Science* **1998**, *281*, 389−392.
(15) Storhoff, J. J.; Mirkin, C. A. *Chem. Rev.* **1999**, *99*, 1849−1862.
(16) Niemeyer, C. M. *Angew. Chem., Int. Ed.* **2001**, *40*, 4128−4158.
(17) Park, S.-J.; Lazarides, A. A.; Mirkin, C. A.; Letsinger, R. L. *Angew. Chem., Int. Ed.* **2001**, *40*, 2909−2912.
(18) Schneider, J. P.; Pochan, D. J.; Ozbas, B.; Rajagopal, K.; Pakstis, L.; Kretsinger, J. *J. Am. Chem. Soc.* **2002**, *124*, 15030−15037.
(19) Xing, B.; Yu, C.-W.; Chow, K.-H.; Ho, P.-L.; Fu, D.; Xu, B. *J. Am. Chem. Soc.* **2002**, *124*, 14846−14847.
(20) Nowak, A. P.; Breedveld, V.; Pakstis, L.; Ozbas, B.; Pine, D. J.; Pochan, D.; Deming, T. J. *Nature* **2002**, *417*, 424−428.

10.1021/ja035211t CCC: $25.00

nanoparticle populations having different sequences are mixed. As long as the DNA sequences are not complementary, the nanoparticles do not cluster in solution. However, addition of a free DNA strand that is complementary to *both* populations causes aggregation of the nanoparticles into cross-linked network structures. Alternatively, one DNA sequence is attached to nanoparticles while a second is functionalized with biotin and attached to the tetrafunctional protein avidin. Addition of the bridging oligonucleotide leads to assembly of nanoparticle-protein composite networks.[17] While this technology has a number of interesting and useful properties, it is not ideal for our purposes because it lacks complete control over the number of potential cross-linking sites (i.e., DNA strands) on each nanoparticle.

Tirrell and co-workers recently reported the design of a biopolymer gel using recombinant DNA technology to engineer bacteria to express proteins having self-assembling units.[14] The strict requirements of the genetic code ensure that the molecular weight distribution of the protein is monodisperse and that the recognition elements are always found in the same place in every copy of the protein produced. The proteins were designed such that the polypeptide chain would spontaneously fold into regions of α-helical secondary structure. These α-helices could then further assemble into coiled-coil tertiary structures in which two or more α-helices wrap around one another to form a bundle.[21] This could occur in either intra- or intermolecular arrangements, with the latter leading to a cross-linked gel since each protein contained multiple α-helices. While the well-defined number and placement of cross-linking elements in this system were attractive, we perceived two disadvantages to this design in terms of studying the internal structure of the gel. First, the potential for forming intramolecular cross-links complicates the system. Second, the stability of the coiled-coil motif cannot be adjusted as easily as the base pairing scheme offered by DNA, where addition and subtraction of base pairs or alteration of base sequence can be used to sensitively adjust the gelation temperature over a very broad range.

The tripartite system we designed combines well-defined functionality with fine control over the gelation temperature to produce micron-sized particles. A combination of optical spectroscopy and laser light scattering was used to study both the assembly process and internal structure of the aggregates. The thermoreversible assembly of the "microgels" is well described by a cluster−cluster aggregation model, as evidenced by fractal analysis of the internal structure of the cross-linked network.

Experimental Section

Materials. Synthetic DNA oligonucleotides (250 nanomole scale, purified by gel filtration chromatography) were purchased from Integrated DNA Technologies, Inc.(www.idtdna.com) as lyophilized powders and used without further purification. Specific base sequences are given at the appropriate points in the Results section. DNA solutions were prepared in 10 mM aqueous sodium phosphate buffer (pH = 7.0) and stored at −4 °C. Concentrations were determined by UV absorbance at 260 nm using molar extinction coefficients calculated using the Schepartz' lab biopolymer calculator (http//paris.chem.yale.edu/extinct.html).

Avidin was obtained from Molecular Probes, Inc (www.probes.com), and solutions were prepared by dissolving 1 mg of avidin in 500 μL of deionized water. Concentrations were determined by UV−vis using a Varian Cary 3 Bio UV−visible spectrophotometer, interfaced to a Dell personal computer for data collection and analysis (using Varian software). The cell path lengths were 1 cm, and the cell holder was maintained at a constant temperature (25 °C). The extinction coefficient for avidin is $\epsilon_{282} = 96\,000\ M^{-1}\ cm^{-1}$.[22] PNA monomers were purchased from Applied Biosystems (www.pebio.com). 6-(Boc-amino)caproic acid and biotin were from Aldrich.

PNA oligomers were synthesized on a lysine-functionalized MBHA resin using standard solid-phase PNA synthetic protocols.[23,24] Biotin was added to the N-terminus of the PNA as the last step in the synthesis, following addition of the 6-aminocaproic acid linker. The crude product was purified by reversed-phase HPLC and characterized by MALDI-TOF mass spectrometry using sinapinic acid as a sample matrix (observed, 2416.8 g/mol; calculated, 2415.4 g/mol). The corresponding PNA without biotin (but with 6-aminocaproic acid) on its N-terminus was also synthesized (observed, 2192.2 g/mol; calculated, 2189.2 g/mol). PNA stock solutions were prepared in deionized water and stored at −4 °C. Concentrations were determined by measuring UV absorbance at 260 nm at 80 °C, where the nucleobases are assumed to be unstacked, and extinction coefficients were calculated by summing the values for the individual nucleobases.

Microgel Formation. Three-way junctions (TWJs) were prepared by mixing the appropriate DNA strands in a buffer containing 250 mM NaCl, 10 mM NaPi, and 0.1 mM EDTA at pH 7.0. The concentration of DNA was 2 μM of each strand. The DNA strands were annealed into junctions by heating the solutions at 75 °C for 5 min and then slowly cooling to 5 °C at a rate of 1 °C/min. A similar procedure was followed with 6 μM PNA to prepare the biotinylated TWJ. Melting curves were measured by monitoring the absorbance at 260 nm while the temperature was increased at a rate of 1.0 °C/min, with data collected every 0.5 °C. To cross-link the TWJ elements into a microgel, avidin was added to the biotinylated TWJ and the sample was allowed to incubate at room temperature for at least 1 h.

Fluorometric Analysis of Biotin−Avidin Binding.[25] A standard solution of biotin (1.0 mg/mL) was prepared by dissolving 50 mg of biotin in 50 mL of 150 mM aqueous NaPi followed by dilution to 20 μg/mL (81.9 μM). For titrations of the biotinylated TWJ into avidin, a stock solution containing 27.3 μM TWJ and 81.9 μM biotinylated PNA was prepared according to the annealing procedure described above. Alternatively, solutions were prepared containing either 27.3 μM TWJ with the nonbiotinylated PNA hybridized or containing 81.9 μM free biotin. A 3.6 μM avidin solution was titrated with successive 1.0 μL aliquots of the appropriate stock solution, and fluorescence was measured at 350 nm with excitation at 290 nm. Additions were made until no further decrease in fluorescence was observed, indicating the attainment of the saturation point.

Laser Light Scattering. All laser light scattering experiments were performed with a Spectra Physics Model 2020 Argon Ion Laser operating at a wavelength of 514.5 nm. The intensity of scattered light and the intensity autocorrelation function were obtained with a Brookhaven Instruments model 9000 digital correlator. A Brookhaven Instruments model BI-240 goniometer was used to set the scattering angle with a vernier scale. The sample cell was placed in a temperature-controlled index-matching vat that was connected to a Lauda model RM-6 constant temperature circulator (±0.5 °C). The circulating bath was filled with water, and the measurements were carried out in the range 10−55 °C. Both avidin and biotinylated TWJ solutions were filtered (Whatman, 0.2 μm) to eliminate dust. Avidin solutions were dripped into biotinylated TWJ solutions very slowly during the filtering

(21) Crick, F. H. C. *Acta Crystallogr.* **1950**, *6*, 689−697.
(22) Bayer, E. A.; Wilchek, M. *Methods Biochem. Anal.* **1980**, *26*, 1−39.
(23) Christensen, L.; Fitzpatrick, R.; Gildea, B.; Petersen, K. H.; Hansen, H. F.; Koch, T.; Egholm, M.; Buchardt, O.; Nielsen, P. E.; Coull, J.; Berg, R. H. *J. Pept. Sci.* **1995**, *3*, 175−183.
(24) Koch, T. In *Peptide Nucleic Acids*; Nielsen, P. E., Egholm, M., Eds.; Horizon Scientific Press: Norfolk, U.K., 1999; pp. 21−37.
(25) Lin, H. J.; Kirsch, J. F. *Anal. Biochem.* **1977**, *81*, 442−446.

Table 1. Parameters for Microgel Components

particle	MW (g mol^{-1})	temp (°C)	concn (μM)	R_h (nm)
avidin	66 000	20.0−55.0	8.0−24	3.5 ± 0.2
AByP	75 667	20.0−55.0	8.0−24	3.7 ± 0.4
biotinylated TWJ	33 841	25.0	12−24	3.7 ± 0.5

process. The aggregated molecules were heated to 5 °C above the complete dissociation temperature for the DNA/PNA junctions for 3 h to erase the thermal history before reversible investigation. Both heating and cooling rates were 0.1 °C/min, and the samples were incubated at the desired temperature for 2−3 h before data collection. In static light scattering (SLS) experiments, the scattering angle was in the range 30−90° with 10° intervals. The excess scattered intensity was calculated after blank and scattering volume calibration.

SLS measures the time-averaged intensity of scattered light, $\langle I_s(q,t)\rangle$, where q is called the scattering vector.[26,27] The magnitude of the scattering vector is given by

$$q = \frac{4\pi n}{\lambda}\sin\left(\frac{\theta}{2}\right) \quad (1)$$

where λ is the wavelength of the incident light, n is the refractive index of the scattering medium, and θ is the scattering angle. Light scattering by particles in solution is characterized by a scattering function, $S(q)$, that depends on the size and structure of the particles. (See Supporting Information for more details.) One important measure of the particle size is the radius of gyration R_g. When $qR_g \ll 1$, the scattering function can be expressed as

$$S(q) = 1 - \frac{(qR_g)^2}{3} \quad (2)$$

If the particles have a self-similar (i.e., fractal) internal structure, the scattering function in the limit that $qR_g \gg 1$ takes the form

$$S(q) \approx q^{-d_f} \quad (3)$$

where d_f is called the fractal dimension of the structure.[28,29]

Fluctuations of the scattering intensity come from fluctuations of the concentration due to the Brownian motion of the scatterers.[30] In dynamic light scattering (DLS) experiments, the intensity autocorrelation function is measured and used to obtain the single particle Brownian diffusion coefficient D_0.[31,32]

$$D_0 = \frac{k_B T}{6\pi\eta R_h}$$

where η is the solvent viscosity and R_h is the hydrodynamic radius of the particle. (See Supporting Information for more details.)

The hydrodynamic radii (R_h) of avidin, avidin/biotinylated PNA complex (AByP, where four biotinylated PNA strands are bound to each avidin), and biotinylated TWJ in buffer were measured by DLS in dilute solution. The R_h (Table 1) of the small particles did not change with concentration in the detection range. All particles had a similar R_h, between 3.5 and 3.7 nm. The R_h values of avidin and AByP were also measured over a wide temperature range. No shift in the sizes of the particles was observed when the temperature was increased from 20.0 to 55.0 °C. Thus, the biopolymers did not undergo denaturation during heating and cooling experiments.

When the solution contains a mixture of particles, the intensity autocorrelation function can be analyzed using the method of non-negatively constrained least squares (NNLS) to obtain a distribution of particle sizes. (See Supporting Information for more details.)

Results

Design of a Thermoreversible Biopolymer Microgel. A thermally reversible gel is most readily prepared from components that are held together through noncovalent cross-links. In addition, at least one of the components involved in forming the gel must be at least trifunctional. Our system is comprised of three distinct components. First, three partially complementary DNA strands assemble spontaneously into a three-way junction through Watson−Crick hydrogen bonding (Figure 1). Lilley and co-workers demonstrated through fluorescence resonance energy transfer (FRET) experiments that the junction shown in Figure 1 adopts a symmetrical Y-shaped structure, on average.[33] At the end of each arm of the junction is a single-stranded overhang having the sequence 5′-AACTCTA-3′; these serve as points of attachment for the second component, which is a biotinylated peptide nucleic acid (PNA) oligomer. PNA is a synthetic analogue of DNA in which the natural phosphodiester backbone is replaced with a polyamide.[34−37] PNA binds with high affinity to complementary DNA sequences according to the Watson−Crick rules.[38] The high thermodynamic stability of the resulting PNA−DNA duplexes allows us to use relatively short sequences, which, in turn, allows us to easily tune the gelation temperature (vide infra). Finally, the third component is the tetrameric protein avidin, which possesses four discrete, high affinity ($K_d = 10^{15}$ M^{-1}) binding sites for biotin.[39] Thus, the biotinylated PNA links each avidin protein to as many as four three-way junctions, ultimately leading to formation of a cross-linked, network structure. At high concentrations, this assembly would form a gel, but at the concentrations used for our experiments and based on the light scattering experiments described below, it is more appropriate to refer to the structures as microgels. The value of introducing the biotinylated PNA rather than simply placing biotin directly onto the arms of the three-way junction lies in the versatility of varying the overhang sequences to shift the gelation temperature, without affecting the stability of the junction.

PNA−DNA Hybridization. We first used temperature-dependent UV−vis spectroscopy to characterize the thermal stability of the biotin-PNA/TWJ system in the absence of avidin. Figure 2 illustrates melting curves for the TWJ alone (solid line) and with the biotinylated PNA present (dashed line). As the temperature is raised, an increase in absorbance is observed due to unstacking of the nucleobases and disruption of the hydrogen bonds holding the different strands together. In the absence of

(26) Berne, B.; Pecora, R. *Dynamic Light Scattering*; Academic Press: New York, 1974.
(27) Chu, B. *Laser Light Scattering*; Academic Press: New York, 1991.
(28) Rothschild, G. W. *Fractals in Chemistry*; John Wiley & Sons: New York, 1998.
(29) Birdi, K. S. *Fractals in Chemistry, Geochemistry and Biophysics*; Plenum: New York, 1993.
(30) Johnson, S. C.; Gabriel, A. D. *Laser Light Scattering*; Dover Publications: New York, 1981.
(31) deGennes, P. G. *Scaling Concepts in Polymer Physics*; Cornell University Press: New York, 1979.
(32) Kim, S. H.; Ramsay, D. J.; Patterson, G. D. *J. Polym. Sci., Part B: Polym. Phys.* **1990**, *28*, 2023−2056.
(33) Stuhmeier, F.; Welch, J. B.; Murchie, A. I. H.; Lilley, D. M. J.; Clegg, R. M. *Biochemistry* **1997**, *36*, 13530−13538.
(34) Nielsen, P. E.; Egholm, M.; Berg, R. H.; Buchardt, O. *Science* **1991**, *254*, 1498−1500.
(35) Nielsen, P. E.; Haaima, G. *Chem. Soc. Rev.* **1997**, *26*, 73−78.
(36) Nielsen, P. E. *Pure Appl. Chem.* **1998**, *70*, 105−110.
(37) Uhlmann, E.; Peyman, A.; Breipohl, G.; Will, D. W. *Angew. Chem., Int. Ed.* **1998**, *37*, 2796−2823.
(38) Green, N. M. *Biochem. J.* **1963**, 585−591.
(39) Egholm, M.; Buchardt, O.; Christensen, L.; Behrens, C.; Freier, S. M.; Driver, D. A.; Berg, R. H.; Kim, S. K.; Nordén, B.; Nielsen, P. E. *Nature* **1993**, *365*, 566−568.

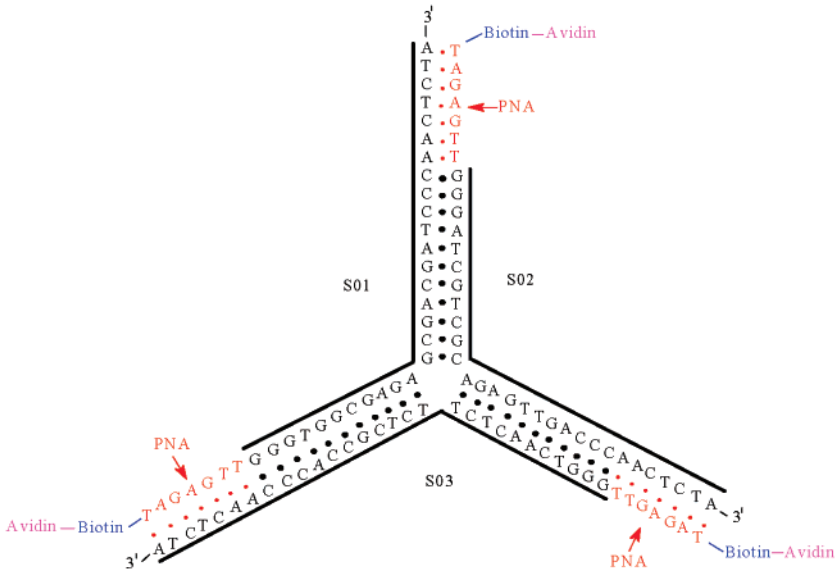

Figure 1. Molecular design of a cross-linked network structure based on a DNA TWJ. Note that each avidin protein can bind four biotinylated TWJ assemblies, leading to the network structure.

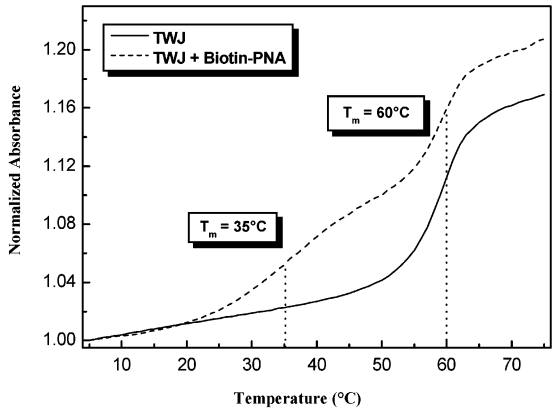

Figure 2. UV−melting curve of DNA TWJ and TWJ + biotinylated PNA. Samples contained 2.0 μM concentrations of each DNA strand with (dashed) and without (solid) 6.0 μM PNA. Data were collected by monitoring the absorbance at 260 nm while heating was at a rate of 1.0 °C/min.

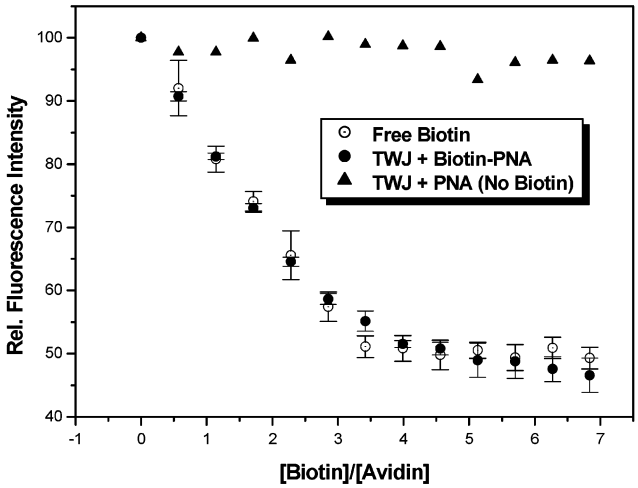

Figure 3. Fluorescence titrations of avidin by biotin (open circles), biotinylated TWJ (filled circles), and nonbiotinylated TWJ (filled triangles). [Avidin] = 3.6 μM in buffer. Samples were excited at 290 nm, and the fluorescence intensity was measured at 350 nm.

PNA, a single transition is observed with a midpoint temperature (T_m) of 60 °C, determined from the maximum of the first derivative of the melting curve. This transition corresponds to the cooperative dissociation of all three strands of the TWJ. In the presence of the PNA, the transition at 60 °C is still observed but, in addition, a lower temperature transition is evident with T_m = 35 °C. We assign the lower transition to disruption of the PNA−DNA duplex at the ends of the TWJ arms, while the upper transition is due to dissociation of the TWJ into its individual strands.

Biotin−Avidin Interaction. Each subunit of the tetrameric avidin protein contains tryptophan residues in the biotin-binding pocket. The fluorescence from these aromatic residues is partially quenched upon binding of biotin, an effect which is useful not only for detecting binding but also for determining how many binding sites are actually occupied by biotin at saturation.[25] This was an important consideration in our system since the different symmetries of the tetrafunctional avidin and trifunctional TWJ might sterically preclude biotin binding to all four sites on the protein. Three separate titration experiments are illustrated in Figure 3. When free biotin is titrated into an aqueous suspension of avidin, the fluorescence is progressively quenched. The saturation point is assigned to a 4:1 ratio of biotin:avidin and is considered to be an accurate method for determining actual avidin concentrations in solution.[25] If the same experiment is performed using the TWJ with biotinylated PNA hybridized to each arm, the quenching follows a nearly identical concentration dependence. This indicates that (*i*) appending the biotin to the TWJ does not significantly weaken the affinity of its binding to avidin and (*ii*) all four binding sites on avidin readily bind to biotinylated three-way junctions. In contrast, if a PNA having identical sequence but lacking the terminal biotin unit is used, no quenching is observed.

Dynamic Light Scattering Reveals Formation of a Microgel. We next used dynamic light scattering (DLS) to estimate the size of the structures formed when avidin is mixed with the biotinylated TWJ. At temperatures below 48 °C, the distribution of particle sizes showed two peaks. Figure 4 presents the distributions obtained at different temperatures. The ordinate is the intensity-weighted amplitude associated with decay

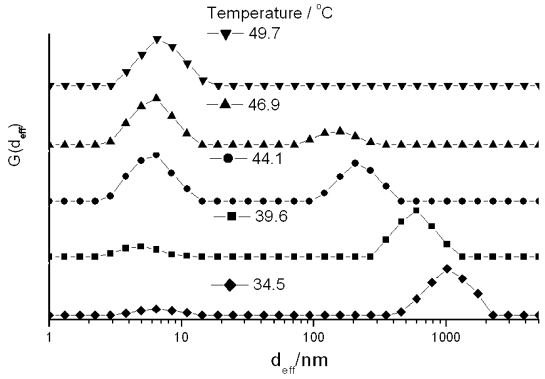

Figure 4. Distribution of the effective diameter in a 6.0 μM avidin + biotinylated TWJ solution at different temperatures; DLS scattering angle is 90°.

components that correspond with scattering by particles of hydrodynamic size (effective diameter) $d_{\text{eff}} = 2R_{\text{h}}$. The peak centered at d_{eff} values between 6 and 7 nm corresponds to the isolated components (Table 1). As the temperature is lowered, a second peak appears and shifts progressively to a larger d_{eff}, reaching 1 μm diameter at the lowest temperature. This peak is well-defined throughout the temperature range, indicative of a relatively narrow distribution of sizes for these *microgel* particles. Extended annealing at the same temperature and temperature cycling that returned to the original temperature gave distributions that were nearly identical. This result emphasizes the equilibrium nature of the distributions and the reversibility of the microgel association. Cooling below 35 °C leads to aggregation and precipitation of the microparticles, although heating and shaking results in redistribution to isolated particles. The average size of the microgel particles is determined by a thermodynamic balance of the enthalpy and entropy of the DNA−PNA binding and the entropy determined by the number of microgel particles (see Discussion).

Static Light Scattering Reveals the Fractal Nature of the Microgels. Static light scattering (SLS) was next used to follow the association and melting of the microgels and to investigate the internal structure of the microgels. We prepared samples by mixing the components at room temperature then heating the mixture to 52.5 °C. This is above the temperature at which the microgel dissociates based on the DLS results (Figure 4) but below the melting temperature of the DNA TWJ (Figure 2). As the sample cools, the microgels reassemble, and this process is easily monitored by SLS. Figure 5A shows the angular dependence of the reduced scattering intensity at fixed temperatures during the cooling process. At high temperatures, the scattering intensity was almost independent of scattering angle, which denoted that there were only small particles in the solution. As the temperature decreased, the small particles reassociated to form large clusters whose structure factor resulted in the appearance of an angular dependence to the scattering intensity. At the lowest temperatures, the relative intensity had the same angular dependence, even though the DLS results indicated that the average particle size was still increasing. This behavior is a signature for the presence of scattering by fractal structures. If the slope of the plot for the lowest temperatures is interpreted in terms of eq 3, the fractal dimension of the internal structure of the largest microgels was approximately 1.85. [40,41]

The microgel can dissolve once more by heating to disrupt the PNA/DNA double helix. We studied the reversibility of this process by SLS. A convenient measure to follow this process was the relative intensity at a fixed angle. The results during both cooling and heating are shown in Figure 5b. The data obtained during heating are within the experimental error of those obtained during cooling; therefore, the microgelation process is truly thermoreversible.

Tuning the Gelation Temperature. In our system, gelation requires only hybridization of the complementary PNA and DNA strands. In principle, one should be able to shift the gelation temperature in a controlled fashion simply by varying the length and/or sequence of the PNA−DNA duplex as this changes the number of hydrogen bonds and the degree of π stacking holding the two strands together. To test this, we studied two additional systems by SLS (Table 2). In the first, a single mutation was introduced into the DNA overhangs, resulting in an A−A mismatch. The loss of hydrogen bonding at this site should destabilize the PNA−DNA duplex, resulting in a lower gelation temperature. The second variation tested involved the same A−A mismatch as well as deletion of the last base on the DNA overhang. In this case, the duplex would only have five base pairs in addition to the terminal A−A mismatch. Moreover, the mismatch is at the very end of the duplex, rather than at the penultimate position; SantaLucia and co-workers have shown such mismatches to be particularly destabilizing in the context of DNA−DNA duplexes,[42] so an even greater shift to lower temperature was expected for gelation of this system.

Figure 6 shows the SLS results for these systems, along with the data for the fully matched sequence shown previously. In each case, the gelation is completely thermoreversible and the gelation temperatures respond to the sequence alterations as expected. The microgel formed from the single mismatch sequence melts 3 °C below the fully matched sequence. Meanwhile, the sequence containing both a mismatch and a deletion melted at 23 °C, approximately 20° lower than the fully matched sequence. These results demonstrate clearly the high degree of control available in designing biopolymer microgels based on Watson−Crick hybridization.

Discussion

The complementary base-pairing rules first elucidated by Watson and Crick[43] are being used to construct a wide variety of nano- and microscale objects and have given birth to a field known as "DNA nanotechnology".[44,45] An interesting recent example of this type of research was reported by Kimizuka and co-workers, who described the spontaneous assembly of DNA three-way junctions (TWJs) into supramolecular cages ranging in diameter between 48 and 275 nm.[46] The cages assembled based on self-complementary sequences extending beyond the base paired arms of the TWJ. In our design, the overhanging sequence on the TWJ was not self-complementary, allowing

(40) Meakin, P.; Wasserman, Z. R. *Phys. Lett.* **1984**, *103A*, 337−341.
(41) Meakin, P. *Phys. Rev. Lett.* **1983**, *51*, 1119−1122.
(42) Peyret, N.; Seneviratne, P. A.; Allawi, H. T.; SantaLucia, J., Jr. *Biochemistry* **1999**, *38*, 3468−3477.
(43) Watson, J. D.; Crick, F. H. C. *Nature* **1953**, *171*, 737−738.
(44) Seeman, N. C. *Annu. Rev. Biophys. Biomol. Struct.* **1998**, *27*, 225−248.
(45) Niemeyer, C. M. *Angew. Chem., Int. Ed.* **2001**, *40*. 4128−4158.
(46) Matsuura, K.; Yamashita, T.; Igami, Y.; Kimizuka, N. *Chem. Commun.* **2003**, 376−377.

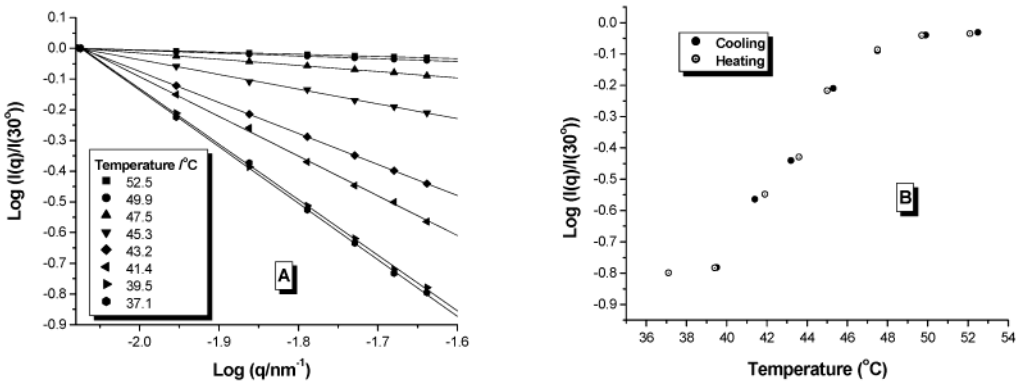

Figure 5. Thermoreversible gelation in a 6.0 μM avidin + biotinylated TWJ solution analyzed by static light scattering. (A) log−log plot of scattering intensity as a function of scattering vector q for several temperatures. (B) Relative intensity at a fixed angle, 90°, as a function of temperature.

Table 2. Sequence Variations for Tuning the Gelation Temperature[a]

hybrid	sequence	gelation temp, °C
fully matched	DNA: 5′-AACTCTA-3′ PNA: Lys-TTGAGAT-Bio	43
single mismatch	DNA: 5′-AACTC***A***A-3′ PNA: Lys-TTGAG***A***T-Bio	40
single mismatch plus deletion	DNA: 5′-AACTC***A***- -3′ PNA: Lys-TTGAG***A***T-Bio	23

[a] Mismatch and deletion positions are underlined (Bio = Biotin).

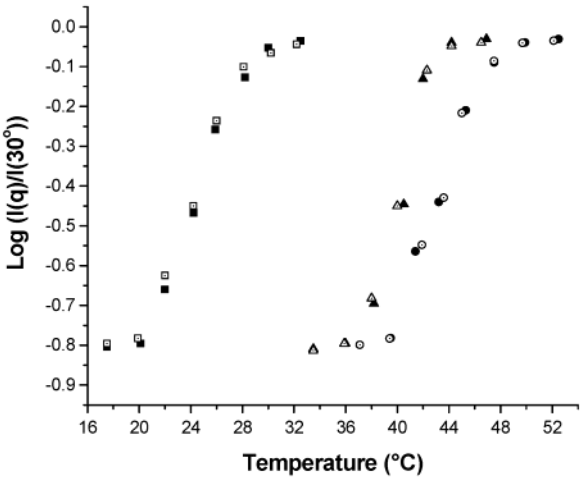

Figure 6. Effect of PNA−DNA sequence on gelation temperature in 6.0 μM avidin + biotinylated TWJ solutions. Filled and open symbols correspond to cooling and heating runs, respectively. Circles: Fully matched sequence. Triangles: Single mismatched sequence. Squares: mismatched + deletion sequence. (Relative intensity observed at 90°.)

us to assemble the microgels using three independent molecular recognition steps: (*i*) hybridization of the three DNA strands to form the TWJ, (*ii*) hybridization of the biotinylated PNA onto the single-stranded ends of the TWJ, and (*iii*) binding of the biotinylated TWJ to avidin. The UV−melting curves shown in Figure 2 demonstrate the first two recognition events, while the fluorescence data shown in Figure 3 verify the third event. The latter data indicate that the affinity of the biotin−avidin interaction is unchanged by attachment of the biotin to the TWJ and that all four binding sites on avidin are occupied at saturation. This may seem surprising, given the trifunctional nature of the biotinylated TWJ and the tetrafunctional nature of avidin. Furthermore, the four biotin-binding sites on avidin are not symmetrically distributed on the protein surface but rather are arranged in pairs on opposite sides of the protein. It is likely that the long, flexible 6-aminocaproic acid linker connecting the biotin to the N-terminus of the PNA oligomer relieves any strain associated with assembling the microgel from these geometrically mismatched components. However, we cannot rule out the possibility that some fraction of the PNA−DNA hybrids are disrupted in order to permit the much higher affinity biotin−avidin interaction to occur. This is the equivalent of introducing defects into the microgel. It will be interesting to use DNA units of different functionalities such as duplex or four-way junctions to study this issue in greater detail.

Dynamic light scattering experiments reveal the formation of micron-sized particles at low temperatures. In particular, the data in Figure 4 indicate that, at temperatures below 40 °C, the particles are sufficiently large to meet the requirement for fractal analysis that $R_g q \gg 1$, as described in the Experimental Section. The calculated fractal dimension (1.85) suggests that the microgel particles have a loose network structure. This structure is consistent with the mechanism of microgel formation. At the highest temperatures, the solution consists of a random mixture of tetrafunctional avidin/biotinylated PNA molecules and trifunctional DNA TWJ molecules. When the temperature is low enough that PNA−DNA junctions can form, the two complementary species can form chains of alternating units that can branch at random locations. The growing loose clusters can then encounter other clusters and link together. This growth mechanism will produce a loose network. Theoretical studies[47−50] of particle aggregation that proceeds by a cluster−cluster aggregation pathway have produced networks with fractal dimensions in the range 1.8−2.0. When all the requirements are satisfied, fractal analysis is a powerful tool in the study of the local structure of the microgels. The three microgels described above differ only in the degree of hydrogen bonding between the PNA and DNA components. The fractal dimension values are essentially identical for all three systems, within experimental error.

The thermoreversibility of our system is well demonstrated by Figures 5 and 6. The microgel dissociates completely at high temperatures due to disruption of the PNA−DNA hybrid. Both the biotin−avidin interaction and DNA TWJ assembly are stable

(47) Meakin, P. *J. Chem. Phys.* **1984**, *81*, 4637−4639.
(48) Martin, J. E.; Hurd, A. J. *J. Appl. Crystallogr.* **1987**, *20*, 61−78.
(49) Jullein, R. *Phys. Rev. Lett.* **1985**, *55*, 1697−1700.
(50) Witten, T. A.; Sander, L. M. *Phys. Rev. Lett.* **1981**, *47*, 1400−1403.

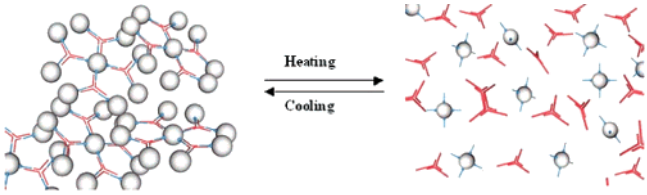

Figure 7. Thermoreversible gelation of tetrafunctional avidin-PNA (spheres) and trifunctional DNA three-way junctions.

under these conditions, and the biotinylated PNA remains associated with the avidin (Figure 7).

At the highest temperatures at which microgel particles are detected, the distribution of particle sizes contains two well-defined peaks. The smaller peak is rigorously demonstrated to be consistent with the individual polyfunctional molecules. At these temperatures, most of the molecules are still free in solution. The presence of a small number of large particles can be explained in detail in terms of the statistics of aggregation of polyfunctional units.[51] Suppose that only 10% of the PNA−DNA junctions have formed. If only linear chains could form, only short sequences would be present, since the relative probability would decrease geometrically with chain length. When the units are polyfunctional, the number of active sites for junction formation actually grows every time a new junction is formed between separate molecules or clusters. The relative probability function now favors large aggregates, since the low probability of individual junction formation is multiplied by the high number of ways of forming the next junction. The ultimate size of the microgel particles is determined by the balance between the overall entropy of the solution and the binding enthalpy of the junctions. Since there is a dynamic equilibrium, the entropy is maximized by having a narrow distribution of large particle sizes. Light scattering is ideally suited to the study of this phenomenon since the intensity depends on the square of the number of subunits in the aggregate. This allows the small number of large aggregates to be seen in the presence of the large number of free molecules. As the temperature is lowered, the fraction of PNA−DNA junctions increases and the number of subunits in the aggregates increases, leading to the larger overall size.

Interestingly, we note that the maximum fractal dimension in our system (ca. 1.85) is considerably lower than that reported by Souza and Miller for their analysis of gold nanoparticle networks held together by DNA cross-links.[52] The apparent fractal dimension reported at similar concentrations to what we used in our experiments was considerably higher. This could be due to the fact that each nanoparticle is capable of forming dozens of cross-links. However, in any analysis of fractal structure, several criteria must be met before valid results can be obtained. First, it is important to fully characterize the monomer particles that will constitute the network so that the angular dependence of the scattering from individual particles does not contribute to the scattering function in the asymptotic range where the fractal dimension dominates. Both static and dynamic light scattering are useful in this characterization. Second, to have a fractal assembly with a well-defined fractal dimension, it is important that many primary particles be contained in the aggregate, such that the overall dimensions of the aggregate are much larger than the individual components. To obtain a valid measure of size for the aggregates, dynamic light scattering is especially useful. Finally, since the fractal aggregates must be large enough that the internal structure can be probed with light scattering, only those data at sufficiently large values of qR_g should be examined on a log−log plot to obtain a valid fractal dimension. The 100 nm diameter gold nanoparticles used in the prior work are large enough that significant angular dependence is expected from the primary particles alone, even prior to formation of a cross-linked network. In addition, the aggregates were reported to be only a few times as large as the primary particles, and the fractal dimension was obtained from the low angle rather than the high angle scattering data. This raises doubts about the values of the fractal dimensions reported for that system.

Finally, the use of Watson−Crick base pairing to assemble the microgels affords the ability to tune the gelation temperature over a wide range and with complete control, as shown in Figure 6. The internal mismatch causes only a slight destabilization of the microgel, while the deletion + terminal mismatch system decreases the gelation temperature by 20 °C. These results indicate that it should be possible to assemble systems in which two or more distinct microgels are present within the same solution but are physically separated from one another due to having noncomplementary sequences. Alternatively, "core−shell" microstructures should form by using subsaturation amounts of one biotinylated PNA/DNA TWJ pair to form the core, followed by addition of a second biotinylated PNA/DNA TWJ pair of different sequence to bind available sites on avidin proteins at the surface of the microgel, with subsequent growth of the particle.

Acknowledgment. This material is based upon work supported by the National Science Foundation under Grant Number DMR-9988451, the Research Seed Fund (Carnegie Mellon), and a Nontenured Faculty Award from 3M Corporation to B.A.A. We thank Guy Berry for helpful discussions. Mass spectra were measured in the Center for Molecular Analysis at Carnegie Mellon University, supported by NSF CHE-9808188.

Note Added after ASAP Posting. The version published on the Web 7/31/2003 did not contain the Supporting Information Available paragraph. The version published on the Web 8/7/2003 and the print version are correct.

Supporting Information Available: Details on light scattering from fractal particles and mixtures of particles. This material is available free of charge via the Internet at http://pubs.acs.org.

JA035211T

(51) Flory, P. J. *Principles of polymer chemistry*; Cornell University Press: New York, 1953.
(52) Souza, G. R.; Miller, J. H. *J. Am. Chem. Soc.* **2001**, *123*, 6734−6735.